European Journal of Computational Mechanics, 2014
Vol. 23, Nos. 1–2, 15–37, http://dx.doi.org/10.1080/17797179.2014.904542

Taylor & Francis
Taylor & Francis Group

A polygonal–FEM technique in modelling arbitrary interfaces on non-conformal meshes: a study on polygonal shape functions

A.R. Khoei*, S.O.R. Biabanaki and R. Yasbolaghi

Center of Excellence in Structures and Earthquake Engineering, Department of Civil Engineering, Sharif University of Technology, P.O. Box. 11365-9313, Tehran, Iran

In this paper, the application of polygonal–FEM method is investigated together with the performance of various polygonal shape functions in modelling of large deformation problems. Polygonal–FEM technique is used in modelling arbitrary interfaces in large deformations using non-conformal meshes. The technique is applied to capture independent deformations in the element cut by the interface in a uniform non-conformal mesh. The geometry of the interface is used to produce various polygonal elements at the intersection of the interface with regular FE mesh, in which the extra degrees-of-freedom are defined along the interface. The level set method is employed to describe the material geometry on the background mesh. Numerical convergence analysis is carried out to study the approximation error and convergence rate of various interpolation functions in polygonal elements. Finally, several numerical examples are solved to investigate the efficiency of each interpolation technique in modelling arbitrary interfaces in large deformations.

Keywords: polygonal–FEM; arbitrary interfaces; large deformations; conforming FEM; pentagonal elements

1. Introduction

In computational mechanics, modelling the arbitrary interfaces on non-conformal meshes is of great importance. The adaptive mesh refinement and conforming mesh strategy for preserving the mesh to the shape of geometry at various stages of solution are time-consuming techniques. Thus, it is necessary to perform an innovative procedure to alleviate these difficulties by allowing the internal interfaces and arbitrary geometries to be mesh-independent. In fact, an approach that avoids the remeshing is preferable not only at the cost of creating a new mesh, but the tremendous overhead associated with adapting post-processing techniques, such as time histories of specified points to sequences of meshes in evolution problems. There are several approaches proposed by researchers to model discontinuity problems with non-conformal meshing, including the mesh-free method (Belytschko, Krongauz, Organ, Fleming, & Krysl, 1996), the generalised finite element method (Strouboulis, Copps, & Babuška, 2001) and the extended finite element method (Belytschko, Moës, Usui, & Parimi, 2001). The extended finite element technique has been extensively employed to minimise the requirement of mesh generation in the problem with material discontinuities, including the hole and inclusion (Sukumar, Chopp, Moës, & Belytschko, 2001), microstructure geometry (Moës, Cloirec, Cartraud, & Remacle, 2003) and arbitrary interfaces (Anahid

*Corresponding author. Email: arkhoei@sharif.edu

& Khoei, 2008; Khoei, Anahid, & Shahim, 2008; Khoei, Biabanaki, & Anahid, 2008), etc. In this method, the enrichment functions are defined to deal with the discontinuity of displacement inside the enriched element. In fact, the method addresses the arbitrary interfaces without generating a boundary-fitted mesh by defining the extra degrees-of-freedom in the elements cut by the interfaces.

Polygonal–FEM technique is a new approach presented in modelling arbitrary interfaces, in which a uniform non-conformal mesh is decomposed into polygonal elements that conform to the internal interfaces and arbitrary geometries. The geometry of interface is used to define the extra degrees-of-freedom by adding nodal points that lie on the interfaces. In order to describe the material geometry on the background mesh, the level set method is employed to represent the decomposition of non-conformal elements into the conformal sub-elements (Noble Newren, & Lechman, 2010). The level set technique is used to extrude any arbitrary geometry from an initial background mesh and model under different external effects. The technique provides a great flexibility in the modelling of complex geometries. The technique may be considered as a generalised finite element method introduced by Li, Lin, and Wu (2003) using a Cartesian Grid with Added Nodes into the unstructured finite elements. In the FE-based Cartesian Grid with Added Nodes method, the additional nodes increase the size of the linear system of equations and significantly affect the structure of the matrix, which make it undesirable compared to other generalised FEM techniques, such as Immersed FE methods. However, in the polygonal finite element method, the polygonal sub-elements are produced in the uniform non-conformal mesh by decomposing the uniform mesh into elements that is conformed to the material interfaces.

The construction of shape functions on irregular polygons were originally proposed by Wachspress (1975) based on the rational basis functions on polygonal elements. In this approach, the principles of perspective geometry of Coxeter (1961) were employed to validate the nodal interpolation and linearity on the boundaries. Various aspects of the Wachspress basis function were investigated in literature, including the estimation of interpolation error on regular hexagons by Gout (1985), the evaluation of polynomial coefficients of Wachspress functions by Dalton (1985), the extension of barycentric coordinate functions to convex polytopes by Warren (1996) and the implementation of higher degree Wachspress functions to construct surface patches by Dahmen, Dikshit, and Ojha (2000), etc. The Wachspress basis function was employed into the finite element method by Dasgupta (2003a, 2003b) to construct the shape functions for concave elements. The construction of conforming finite elements based on polygonal meshes was performed by Sukumar (2004), in which a link between the maximum entropy and the construction of polygonal interpolants was established. In this technique, the maximum entropy approach was used to obtain a feasible solution for the shape functions of convex or non-convex polygons. Sukumar and Tabarraei (2004) proposed the conforming finite elements based on polygonal meshes, which provide a great flexibility in mesh generation of solid mechanics problems. An overview of recent developments in the construction of finite element interpolants based on the C^0–conforming on polygonal domains was presented by Sukumar and Malsch (2006). A numerical integration technique on arbitrary polygonal domains was proposed by Natarajan, Bordas, and Mahapatra (2009) based on the Schwarz–Christoffel conformal mapping. Recently, a polygonal–FEM technique was presented by Biabanaki and Khoei (2012) on the basis of Wachspress shape functions in modelling large deformation problems. A particular and notable contribution of polygonal interpolants is based on the mesh-free, or natural-neighbour, basis functions on a canonical element combined with an affine map to construct conforming approximations

on convex polygons. This numerical formulation enables the construction of conforming approximation on any polygons, and hence extends the potential applications of finite elements to convex polygons of arbitrary order.

In the present study, a new approach is presented based on the polygonal–FEM technique in modelling of large deformations on arbitrary interfaces, in which a uniform non-conformal mesh, such as a quadrilateral grid or a polygonal grid can be decomposed into polygonal elements that conform to the internal interfaces and arbitrary geometries. The conformal FE decomposition technique is performed using various polygonal interpolation functions, in which the polygonal elements are produced in the uniform structured mesh by decomposition of the uniform mesh into sub-elements. The performance of various polygonal shape functions is investigated in large polygonal–FEM deformations, including the Wachspress interpolation, metric coordinates, mean value coordinates and natural neighbours methods. Moreover, the numerical convergence analysis is carried out to study the approximation error and the convergence rate of various interpolation functions for the polygonal–FEM method with quadrilateral and hexagonal meshes. The plan of the paper is as follows: in Section 2, a general formulation is presented for continuum model of large deformation based on the Lagrangian description, which can be used in the standard–FEM, or conforming–FEM technique. Section 3 is devoted to the concept of conforming polygonal finite elements. The implementation of conforming–FEM technique based on the polygonal elements is demonstrated in Section 4. The procedure, in which the polygonal elements are produced in the uniform structured mesh by decomposing the uniform mesh into sub-elements, is described in this section. In Section 5, the numerical convergence analysis is performed to study the approximation error and convergence rate of various interpolation functions in polygonal elements. In addition, several numerical examples are analysed to illustrate the performance of different polygonal interpolation functions in modelling arbitrary interfaces in large deformations. Finally, some concluding remarks are given in Section 6.

2. Large finite element deformation formulation

In non-linear analyses, whether the displacements, or strains, are large or small it is imperative that the equilibrium conditions between the internal and external forces are satisfied. The equilibrium equation of a body in the current deformed configuration can be written in the standard form as

$$\frac{\partial \sigma_{ij}}{\partial x_j} + b_i = 0 \tag{1}$$

where σ_{ij} is the Cauchy stresses, x_j current coordinates and b_i the body force. In order to develop a finite element formulation, we need to solve Equation (1) numerically for spatial discretisation. Following the standard procedure of the finite element method, the initial domain Ω^0 is divided into elements. If the displacements within an element are prescribed by a finite number of nodal values, we can obtain the necessary equilibrium equations using the virtual work principle. Thus, the equilibrium conditions between the internal and external forces, i.e. $W_{\text{int}} = W_{\text{ext}}$ can be written in the following weak form at the initial configuration as

$$\int_{\Omega^0} \delta \boldsymbol{E}^T \boldsymbol{S} d\Omega^0 = \int_{\Omega^0} \delta \boldsymbol{u}^T \boldsymbol{b}^0 d\Omega^0 + \int_{\Gamma_t^0} \delta \boldsymbol{u}^T \bar{\boldsymbol{t}}^0 d\Gamma^0 \tag{2}$$

where $\boldsymbol{E}$ is the Green–Lagrange strain vector and $\boldsymbol{S}$ the second Piola–Kirchhoff stress vector. In above equations, $\boldsymbol{b}$ is the body force vector and $\bar{\boldsymbol{t}}$ the traction applied on the boundaries. The '0' superscript denotes the value of variables according to the undeformed configuration.

In order to formulate the Lagrangian finite element model, the variational equations (2) must be linearised using the Newton–Raphson method. The linearisation of internal work can be obtained in terms of the second PK stresses and Green–Lagrange strains. Since there are two sources of non-linearities in the internal work expression, i.e. the stress vector which depends on the strains, or in turn depends on displacements, and the Green–Lagrange strain vector which is a non-linear function of displacements, the linearisation of internal work can be written as

$$D_{\Delta \boldsymbol{u}} W_{\text{int}} = \int_{\Omega^0} \left(D_{\Delta \boldsymbol{u}} \delta \boldsymbol{E}^T_{(\boldsymbol{u})} \boldsymbol{S}_{(\boldsymbol{u})} + \delta \boldsymbol{E}^T_{(\boldsymbol{u})} D_{\Delta \boldsymbol{u}} \boldsymbol{S}_{(\boldsymbol{u})} \right) d\Omega^0 \tag{3}$$

where $D_{\Delta \boldsymbol{u}} \delta \boldsymbol{E}^T_{(\boldsymbol{u})}$ is the linearisation of variation of the Green–Lagrange strain and $D_{\Delta \boldsymbol{u}} \boldsymbol{S}_{(\boldsymbol{u})}$ is the linearisation of second PK stress. Applying the definition of Green–Lagrange strain and second PK stress and taking their derivatives with respect to Δu, Equation (3) can be rewritten as

$$D_{\Delta \boldsymbol{u}} W_{\text{int}} = \int_{\Omega^0} (\delta \boldsymbol{H}^T \overline{\boldsymbol{S}} \Delta \boldsymbol{H} + \delta \boldsymbol{H}^T \overline{\boldsymbol{F}}^T \boldsymbol{C} \overline{\boldsymbol{F}} \Delta \boldsymbol{H}) d\Omega^0 \tag{4}$$

where $\boldsymbol{C}$ is the 3×3 matrix of tangent elasto-plasticity and $\bar{\boldsymbol{S}}$ is the tensor of second PK stress. In above equation, $\bar{\boldsymbol{F}}$, $\bar{\boldsymbol{S}}$ and $\boldsymbol{H}$ are defined for the plane stress/strain problems as

$$\bar{\boldsymbol{F}}_I = \begin{bmatrix} \partial x_I / \partial X^0 & 0 \\ 0 & \partial x_I / \partial Y^0 \\ \partial x_I / \partial Y^0 & \partial x_I / \partial X^0 \end{bmatrix} \tag{5}$$

$$\bar{\boldsymbol{S}} = \begin{bmatrix} [\boldsymbol{S}] & 0 \\ 0 & [\boldsymbol{S}] \end{bmatrix} \quad \text{with} \quad [\boldsymbol{S}] = \begin{bmatrix} S_{xx} & S_{xy} \\ S_{yx} & S_{yy} \end{bmatrix} \tag{6}$$

$$\boldsymbol{H} = \left\{ \frac{\partial u}{\partial X^0} \frac{\partial u}{\partial Y^0} \frac{\partial v}{\partial X^0} \frac{\partial v}{\partial Y^0} \right\}^T \tag{7}$$

In the linearisation of external work, since there is no effect of displacements on the external work done by the applied forces and body forces, i.e. $D_{\Delta \boldsymbol{u}} \left(\int_{\Omega^0} \delta \boldsymbol{u}^T \boldsymbol{b}^0 d\Omega^0 + \int_{\Gamma^0_t} \delta \boldsymbol{u}^T \bar{\boldsymbol{t}}^0 d\Gamma^0 \right) = 0$, the linearised form of the weak formulation can be written as

$$\int_{\Omega^0} (\delta \boldsymbol{H}^T \bar{\boldsymbol{S}} \Delta \boldsymbol{H} + \delta \boldsymbol{H}^T \overline{\boldsymbol{F}}^T \boldsymbol{C} \bar{\boldsymbol{F}} \Delta \boldsymbol{H}) d\Omega^0 = - \int_{\Omega^0} \delta \boldsymbol{H}^T \overline{\boldsymbol{F}}^T \boldsymbol{S} d\Omega^0 + \int_{\Omega^0} \delta \boldsymbol{u}^T \boldsymbol{b}^0 d\Omega^0 + \int_{\Gamma^0_t} \delta \boldsymbol{u}^T \bar{\boldsymbol{t}}^0 d\Gamma^0 \tag{8}$$

Applying the Lagrangian finite element formulation, the above equation can be obtained as

$$\left(\int_{\Omega^0} \boldsymbol{B}^T\bar{\boldsymbol{S}}\boldsymbol{B}d\Omega^0 + \int_{\Omega^0} \boldsymbol{B}^T\overline{\boldsymbol{F}}^T\boldsymbol{C}\bar{\boldsymbol{F}}\boldsymbol{B}d\Omega^0\right)\Delta\bar{\boldsymbol{u}} = -\int_{\Omega^0} \boldsymbol{B}^T\overline{\boldsymbol{F}}^T\boldsymbol{S}d\Omega^0 + \int_{\Omega^0} \boldsymbol{N}^T\boldsymbol{b}^0 d\Omega^0 + \int_{\Gamma_t^0} \boldsymbol{N}^T\bar{\boldsymbol{t}}^0 d\Gamma^0 \tag{9}$$

where $\boldsymbol{N}$ and $\boldsymbol{B}$ are the shape function and the gradient shape function of the elements, respectively. In Equation (9), the tangential stiffness matrices and load vectors are defined as

$$\begin{aligned}
\boldsymbol{K}_c &= \int_{\Omega^0} \boldsymbol{B}^T\overline{\boldsymbol{F}}^T\boldsymbol{C}\bar{\boldsymbol{F}}\boldsymbol{B}d\Omega^0 \\
\boldsymbol{K}_s &= \int_{\Omega^0} \boldsymbol{B}^T\bar{\boldsymbol{S}}\boldsymbol{B}d\Omega^0 \\
\boldsymbol{R}_{int} &= -\int_{\Omega^0} \boldsymbol{B}^T\overline{\boldsymbol{F}}^T\boldsymbol{S}d\Omega^0 \\
\boldsymbol{R}_t &= \int_{\Gamma_t^0} \boldsymbol{N}^T\bar{\boldsymbol{t}}^0 d\Gamma^0 \\
\boldsymbol{R}_b &= \int_{\Omega^0} \boldsymbol{N}^T\boldsymbol{b}^0 d\Omega^0
\end{aligned} \tag{10}$$

where $\boldsymbol{K}_c$ is the stiffness matrix for large deformation, $\boldsymbol{K}_s$ the stress (or geometric) stiffness matrix, $\boldsymbol{R}_{\text{int}}$ the equivalent load vector due to stresses in the current known configuration, $\boldsymbol{R}_t$ the equivalent nodal load vector due to surface loading and $\boldsymbol{R}_b$ the equivalent nodal load vector due to body force. Thus, Equation (9) can be simplified as

$$\mathbb{K}\Delta\bar{\boldsymbol{u}} = \mathbb{R} \tag{11}$$

where $\mathbb{K} = \boldsymbol{K}_c + \boldsymbol{K}_S$ and $\mathbb{R} = \boldsymbol{R}_{\text{int}} + \boldsymbol{R}_t + \boldsymbol{R}_b$.

3. Interpolation functions in polygonal elements

The most important feature of the finite element method is the ease of covering a body of arbitrary shape with regions of relatively simple geometry. In two-dimensional problems, the typical elements are popular convex polygons, such as triangles and quadrilaterals, which are used in commercial codes to evaluate the domain integrals within finite elements according to numerical quadrature schemes with varied degrees of accuracies. However, the implementation of irregular FE polygons in practical engineering problems has not been significantly explored. The polygonal finite elements provide a great flexibility in modelling of complex geometries, and can be used as the transition elements in FE meshes. Various approaches are proposed by researchers for determining and modifying the interpolation functions in polygonal finite elements, including the Wachspress interpolation, metric coordinates, mean value coordinates and natural neighbours methods. In what follows, a brief overview of these techniques is given.

3.1. Wachspress method

The construction of barycentric coordinates and the evaluation of shape functions on irregular polygons were originally presented by Wachspress (1975) based on the rational basis functions on polygonal elements. The rational barycentric basis functions were enhanced using the GADJ algorithm by Dasgupta (2003a) and Dasgupta and Wachspress (2008), and extended to higher space dimensions by Wachspress (2011). An expression of the Wachspress shape functions was given by Meyer, Barr, Lee, and Desbrun (2002) as

$$N_i^w(\boldsymbol{x}) = \frac{w_i(\boldsymbol{x})}{\sum_{j=1}^{n} w_j(\boldsymbol{x})} \tag{12}$$

where

$$w_i(\boldsymbol{x}) = \frac{A(p_{i-1}, p_i, p_{i+1})}{A(p_{i-1}, p_i, p)A(p, p_i, p_{i+1})} = \frac{\cot\theta_i + \cot\omega_i}{\|\boldsymbol{x}_i - \boldsymbol{x}\|^2} \tag{13}$$

where $A(a,b,c)$ is the signed area of triangle $[a,b,c]$, and θ_i and ω_i are shown in Figure 1. Since $\cot\theta_i + \cot\omega_i \equiv \sin(\theta_i+\omega_i)/(\sin\theta_i \sin\omega_i)$, the shape functions $N_i^w(\boldsymbol{x})$ have non-negative values and the polygon must be convex, i.e. $\theta_i + \omega_i < \pi$. The evaluation of the Wachspress basis function can be carried out using the elementary vector calculus operations, as demonstrated by Meyer et al. (2002). Considering the coordinates of the vertices of triangle (p, p_i, p_{i+1}) as (x_1, x_2), (a_1, a_2) and (b_1, b_2), respectively, the value of $\cot(\omega_i)$ can be computed by

$$\cot\omega_i = \frac{(p_{i+1}-p_i).(p-p_i)}{|(p_{i+1}-p_i)\times(p-p_i)|} = \frac{(b_1-a_1)(x_1-a_1)+(b_2-a_2)(x_2-a_2)}{(b_1-a_1)(x_2-a_2)-(x_1-a_1)(b_2-a_2)} \equiv \frac{C}{S} \tag{14}$$

and its derivatives can be evaluated as

$$\begin{aligned} \frac{\partial(\cot\omega_i)}{\partial x_1} &= \frac{(b_1-a_1)-(a_2-b_2)\cot\omega_i}{S} \\ \frac{\partial(\cot\omega_i)}{\partial x_2} &= \frac{(b_2-a_2)-(b_1-a_1)\cot\omega_i}{S} \end{aligned} \tag{15}$$

The value of $\cot\theta_i$ and its derivatives can be computed in a similar manner. Finally, the Wachspress shape function $N_i^w(\boldsymbol{x})$ can be obtained according to relation (12). In Figure 2(a), the Wachspress shape function of an arbitrary pentagonal element is shown

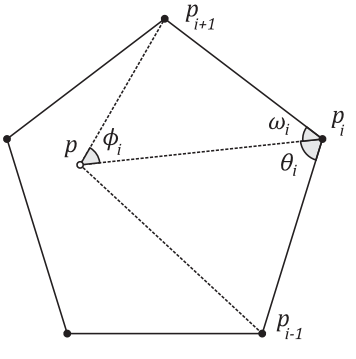

Figure 1. A general polygonal element.

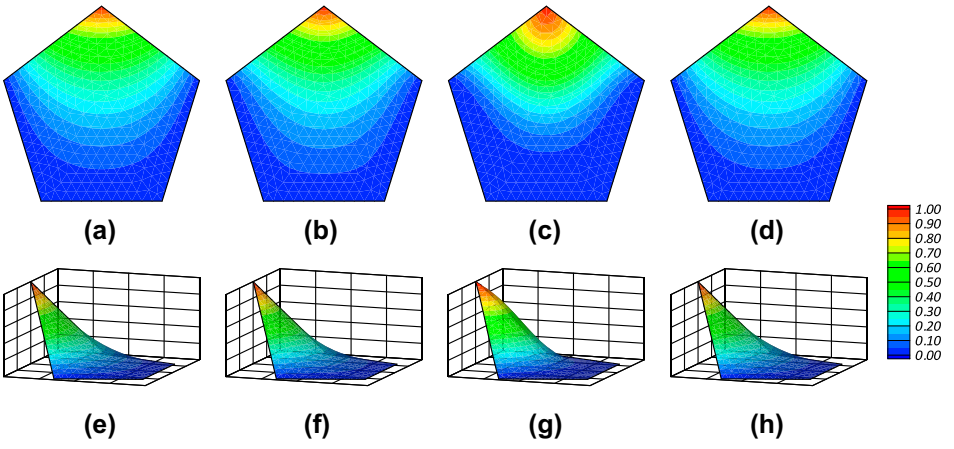

Figure 2. Shape functions of a general pentagonal element; (a, e) Wachspress method, (b, f) mean value method, (c, g) metric method and (d, h) natural neighbours method.

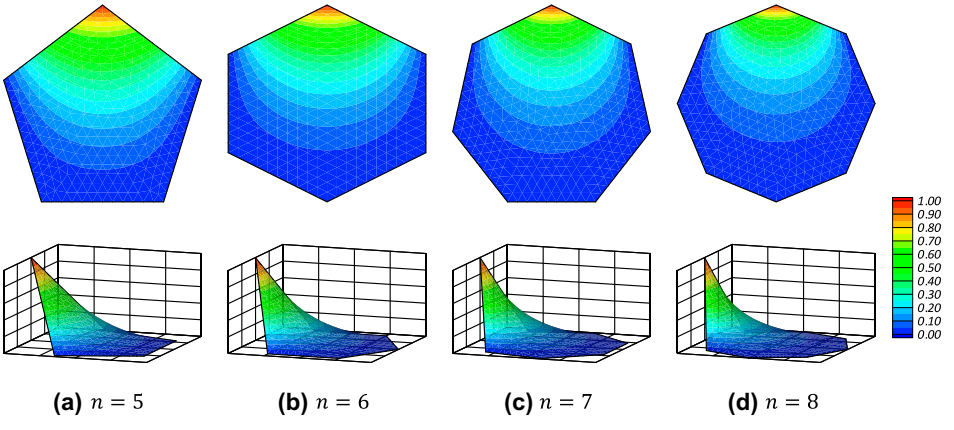

Figure 3. Shape functions of the general polygonal elements.

for the geometry depicted in Figure 1. The Wachspress shape functions of regular polygon ($n-$gon) elements are presented in Figure 3 for four different polygons.

3.2. Mean value coordinates method

The mean value coordinates method was originally proposed by Floater (2003) to interpolate the data in an arbitrary convex or concave domain. This method is based on the mean value theorem used for harmonic functions. The set of interpolation functions constructed by this method satisfies all requirements necessary for obtaining the element shape functions inside of the polygon but it cannot be extended to the boundary of polygonal element. An expression for the shape functions of the mean value coordinates method can be given by

$$N_i^m(\boldsymbol{x}) = \frac{w_i(\boldsymbol{x})}{\sum_{j=1}^{n} w_j(\boldsymbol{x})} \tag{16}$$

where

$$w_i(\boldsymbol{x}) = \frac{\tan(\varphi_{i-1}/2) + \tan(\varphi_i/2)}{\|\boldsymbol{x} - \boldsymbol{x}_i\|} \tag{17}$$

The parameter φ_i is shown in Figure 1. The shape function of a pentagonal element derived by the mean value coordinates method is presented in Figure 2(b).

3.3. *Metric coordinates method*

The metric coordinates method was developed by Malsch and Dasgupta (2004a) and Malsch, Lin, and Dasgupta (2005) in general polygonal domains with convex or concave polygonal element. The method can be employed in the case of multiply connected polygonal domain with isolated points at its interior. The shape functions of the metric coordinates method can be constructed as

$$N_i^r(\boldsymbol{x}) = \frac{w_i(\boldsymbol{x})}{\sum_{j=1}^{n} w_j(\boldsymbol{x})} \tag{18}$$

where

$$w_i(\boldsymbol{x}) = \prod_{j \neq i, i-1} l_j(\boldsymbol{x}) \tag{19}$$

in which $l_j(\boldsymbol{x})$ can be defined for each edge as

$$l_i(\boldsymbol{x}) = \|\boldsymbol{x}_{i-1} - \boldsymbol{x}_i\| - (\|\boldsymbol{x} - \boldsymbol{x}_{i-1}\| + \|\boldsymbol{x} - \boldsymbol{x}_{i-1}\|) \tag{20}$$

The metric shape function of a pentagonal element is shown in Figure 2(c). The metric shape functions are applied in the heat transfer analysis by Malsch and Dasgupta (2004b).

3.4. *Natural neighbours method*

In this approach, the finite elements are introduced based on the Voronoi decomposition of polygonal domain and the interpolation functions are determined using the natural element coordinates. The Voronoi decomposition of a set of nodes in an Euclidean plane is defined as follows; the Voronoi cell associated with node i is defined as the locus of points which are closer to node i than to any other node. The nodes associated with two adjacent Voronoi cells with a common edge are called natural neighbours. In order to calculate a set of finite element interpolation functions based on the natural neighbours method, the Voronoi tessellation is initially determined with respect to the element nodes and interpolation point. The interpolation functions can therefore be defined as

$$N_i^n(\boldsymbol{x}) = \frac{w_i(\boldsymbol{x})}{\sum_{j=1}^{n} w_j(\boldsymbol{x})} \tag{21}$$

where

$$w_i(\boldsymbol{x}) = \frac{\alpha_i(\boldsymbol{x})}{\beta_i(\boldsymbol{x})} \tag{22}$$

where $\beta_i(\boldsymbol{x})$ is the distance between the interpolation point and node i and $\alpha_i(\boldsymbol{x})$ is the length of the common edge of Voronoi cells associated with node i and interpolation point, in which $\alpha_i(\boldsymbol{x})$ is set to zero for the nodes which are not natural neighbours of the interpolation point.

The discrete harmonic mapping functions presented by Pinkall and Polthier (1993) are equivalent to the natural neighbours shape functions. In an arbitrary convex domain, the discrete harmonic weights are defined as

$$w_i(\boldsymbol{x}) = \cot(\theta_i) + \cot(\omega_i) \tag{23}$$

where the angles θ_i and ω_i are shown in Figure 1. The shape function of a pentagonal element derived using the Laplace method is shown in Figure 2(d).

4. Conforming FEM with polygonal elements

In order to model arbitrary interfaces in a uniform mesh, the regular non-conformal mesh is decomposed into sub-elements that conform to the internal interfaces. In this approach, the concept of conformal decomposition finite element method is used to produce the conforming polygonal elements in the uniform structured mesh by decomposition of the uniform mesh into sub-elements that is conformed to the material interfaces. The geometry of interface is used to produce various polygonal elements at the intersection of interface, as shown in Figure 4, in which the extra degrees-of-freedom are defined along the interface. The position of material interface is determined according to the initial uniform mesh by using the level set method.

The level set method is employed to describe the material interface by extruding arbitrary geometry from the initial background mesh. The technique is used to represent the geometry of interface on the structured and non-conformal mesh. The level set method performs the decomposition of non-conformal elements into conformal sub-elements by introducing the material interface based on the sign of level set function.

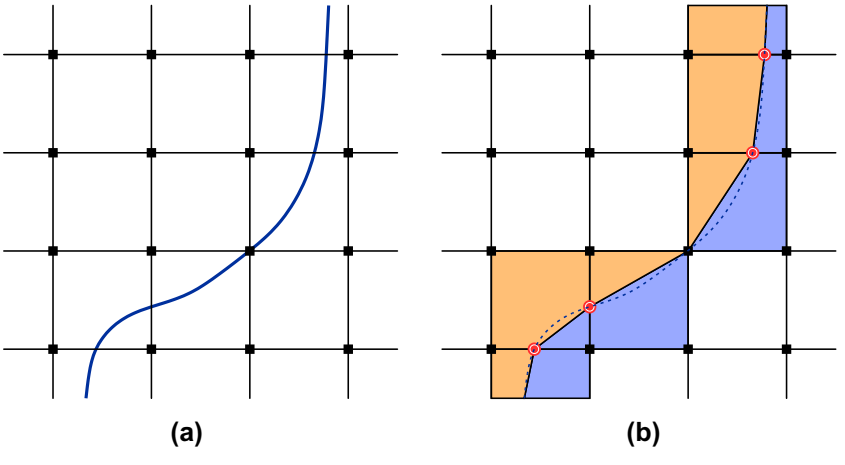

Figure 4. Decomposition of non-conformal elements cut by the interface into conformal sub-elements: ■ original nodal points, ◉ new degrees-of-freedom along the interface.

The performance of this conformal decomposition affects the quality of conformal sub-elements. In general, the conformal decomposition must be robustly handled for unacceptable and degenerate cases. These situations can be occurred whenever the interface passes through a nodal point. In such case, a robust scheme is needed for handling nearly degenerate cases. If nearly degenerate elements are not addressed, the resulting matrix system may be numerically singular.

A general procedure for handling the conformal decomposition can be performed by determination of the edges of non-conformal elements cut by the material interface. An edge is assumed to be cut by the interface if the level set values of two nodal points supported by the edge have different signs. The procedure to handle the nodal points with zero level set values, or nearly zero level set values is optional, but they must be handled consistently. For the edge of element cut by the interface, new degrees-of-freedom are introduced at the edge of non-conformal element, as shown in Figure 4. The coordinates of this point can be obtained by linear interpolation on the edge of element. For an edge with nodal level set values of φ_1 and φ_2, the coordinates of new point can be obtained as

$$\boldsymbol{x}_i = \boldsymbol{x}_1 + \alpha(\boldsymbol{x}_2 - \boldsymbol{x}_1) \tag{24}$$

where $\boldsymbol{x}_1$ and $\boldsymbol{x}_2$ are the coordinates of new point and the value of α is defined by a linear interpolation as $\alpha = ||\varphi_1||/h$, with h denoting the size of element. However, if $\alpha < \varepsilon$, or $\alpha > 1 - \varepsilon$, in which the parameter ε is assumed to be .05, the new point is not generated. In this case, the interface passes through the nearest nodal point of the edge, and the level set value is set to zero at the nearest node. A detailed study of the sensitivity analysis to this decomposition parameter has not been performed here. However, it is obvious that a large value of parameter ε may cause significant errors due to deficiency between the prescribed geometry and the decomposed geometry. In addition, a small value of parameter ε results in multiple nodal points that is numerically coincident.

For the conformal sub-elements, the new point along the interface is added to the original vertex nodal points. Since the new point may be coincident with the vertex nodal points, different cases can be occurred for the conformal sub-elements, as shown in Figures 5–7. As can be observed from these figures, various polygonal elements can be generated according to the position of interface in the regular uniform mesh, including the triangular, quadrilateral and pentagonal elements. If the interface passes through a nodal point, or nearest nodal point ($\alpha < \varepsilon$ or $\alpha > 1 - \varepsilon$), it results in the triangular–quadrilateral sub-elements, as shown in Figure 5(b). If the interface cuts two edges of non-conformal element, the conformal decomposition results in two quadrilateral sub-elements as shown in Figure 5(d), or the triangular–pentagonal sub-elements as shown in Figure 5(f). The conformal decomposition strategy of degenerate cases depends on the path of interface across the edge and nodal points of the element. The conformal decomposition may result in two triangular sub-elements with no new degrees-of-freedom, as shown in Figure 6(d). If the interface passes through the edge of an element, or nearest nodal points of the edge, there is no conformal decomposition and no new degrees-of-freedom, as shown in Figure 7(d). By defining the material interface in the uniform non-conformal mesh and performing the conformal decomposition to generate various polygonal sub-elements, the standard elements and conformal sub-elements within the material zone must be first determined; those elements or sub-elements which are not within the material zone must be then removed, as shown in Figure 8, and the generalised finite element model is finally analysed under the external loading.

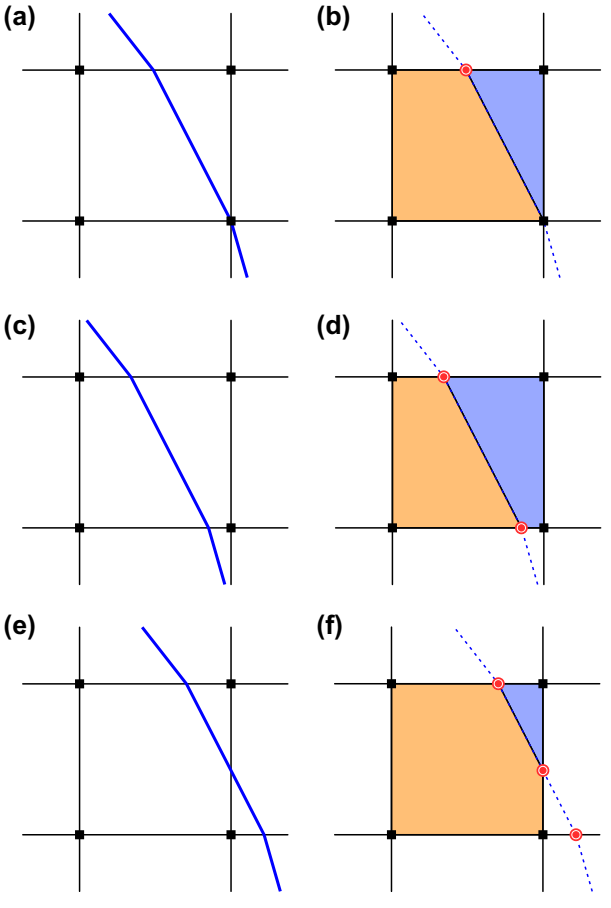

Figure 5. Decomposition of non-conformal element into conformal sub-elements: (a–b) the conformal decomposition with triangular–quadrilateral sub-elements, (c–d) the conformal decomposition with two quadrilateral sub-elements and (e–f) the conformal decomposition with triangular–pentagonal sub-elements.

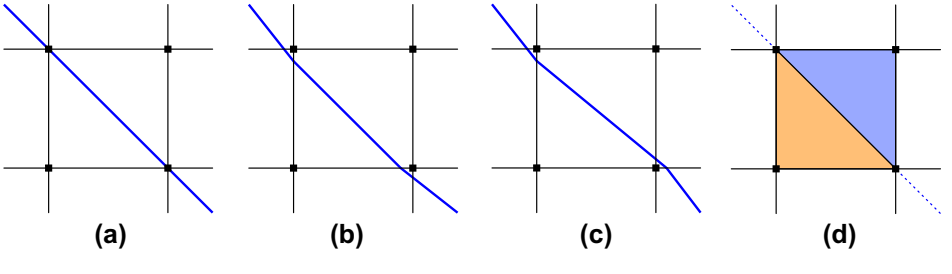

Figure 6. Conformal decomposition with no new degrees-of-freedom: (a–c) the interface passing through the two nodal points, or nearest ones and (d) the conformal decomposition with two triangular sub-elements.

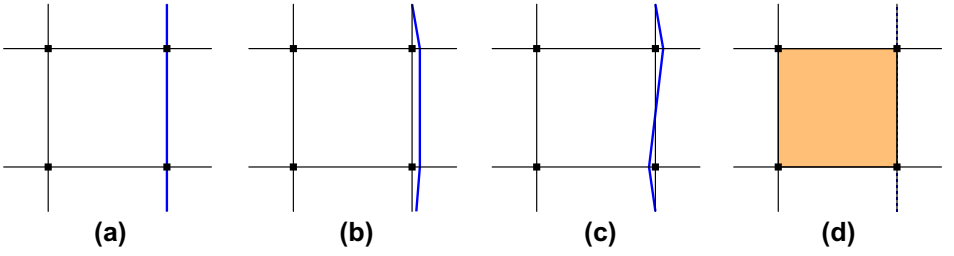

Figure 7. The interface passing through the edge of element, or nearest nodal points of the edge, with no conformal decomposition and no new degrees-of-freedom.

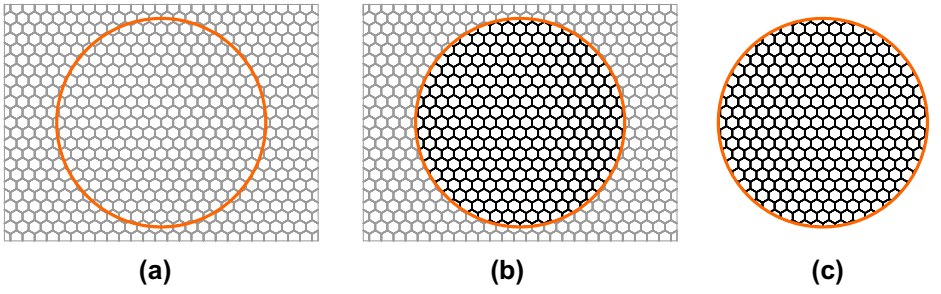

Figure 8. (a) Definition of an interface in the uniform non-conformal mesh, (b) determination of standard elements and conformal sub-elements within the material zone, and (c) elimination of elements not within the material zone.

5. Numerical simulation results

In order to illustrate the accuracy and versatility of the polygonal–FEM technique and to demonstrate the performance of different polygonal shape functions, several numerical examples of free-die pressing with various interfaces, including a plate with an inclined interface, a plate with the flexible central core, a plate with the circular hole and an elastic curved beam are presented. The examples are solved using both the polygonal–FEM and standard–FEM techniques, and the results are compared. In order to perform a real comparison, the same number of elements is assumed for polygonal–FEM and standard–FEM meshes independent of the shape of discontinuity to assess the accuracy of discretisation. All numerical examples are modelled by a plain strain representation and the convergence tolerance is set to 10^{-14}.

5.1. Rectangular plate with inclined internal interface

The first example is chosen to present the convergence study of polygonal–FEM technique using various polygonal interpolation functions. In this example, the evaluation of relative L2 error norm of displacement is obtained for a rectangular plate with inclined internal interface, as shown in Figure 9, and the rate of convergence is compared with the optimal convergence rate. In order to perform the convergence analysis, a comparison is performed between the Wachspress interpolation functions, the metric coordinate shape functions, the natural neighbour-based functions and the mean value coordinate functions. The numerical convergence analysis is carried out for the

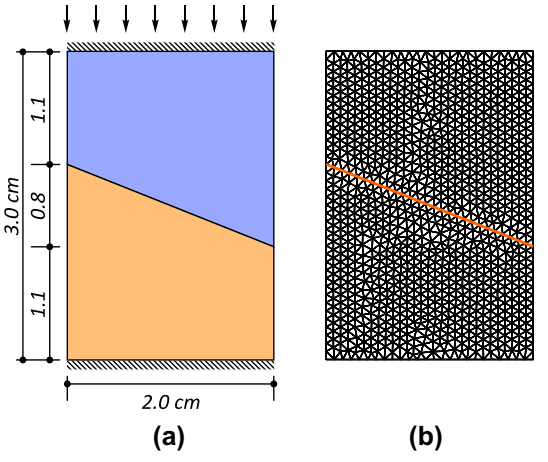

Figure 9. A rectangular plate with an inclined interface: (a) problem definition and (b) the fine FE mesh.

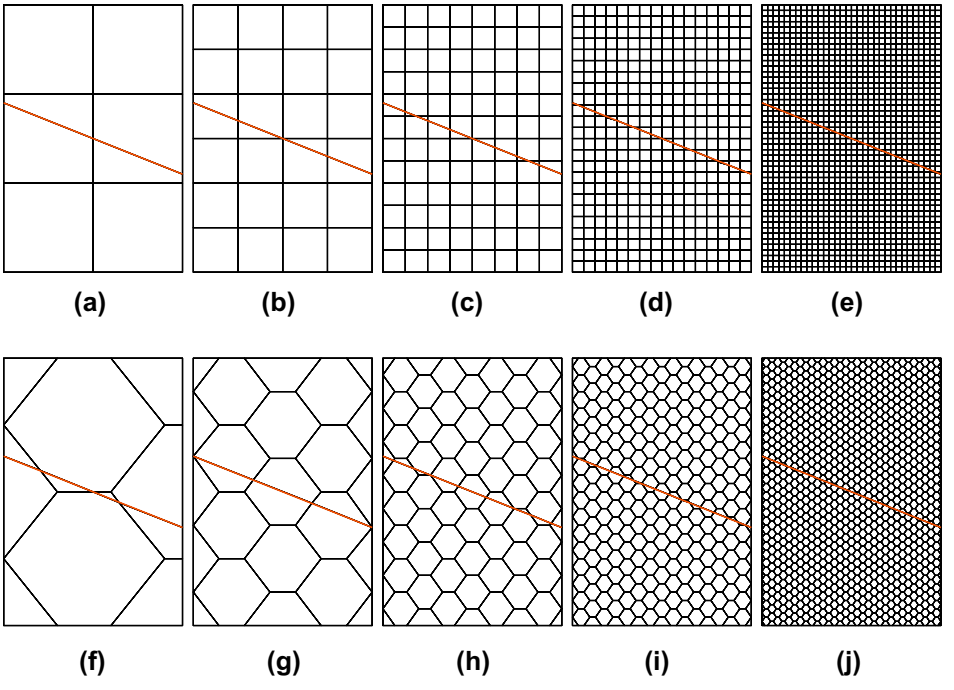

Figure 10. The polygonal finite element modelling of a rectangular plate with inclined interface using various meshes of (a–e) 6, 24, 96, 384 and 1536 quadrilateral elements and, (f–j) 8, 24, 77, 281 and 1073 hexagonal elements.

quadrilateral and hexagonal elements to study the approximation error and convergence rate of various interpolation functions in polygonal elements. For this purpose, various polygonal–FEM meshes of 6, 24, 96, 384 and 1536 quadrilateral elements and 8, 24,

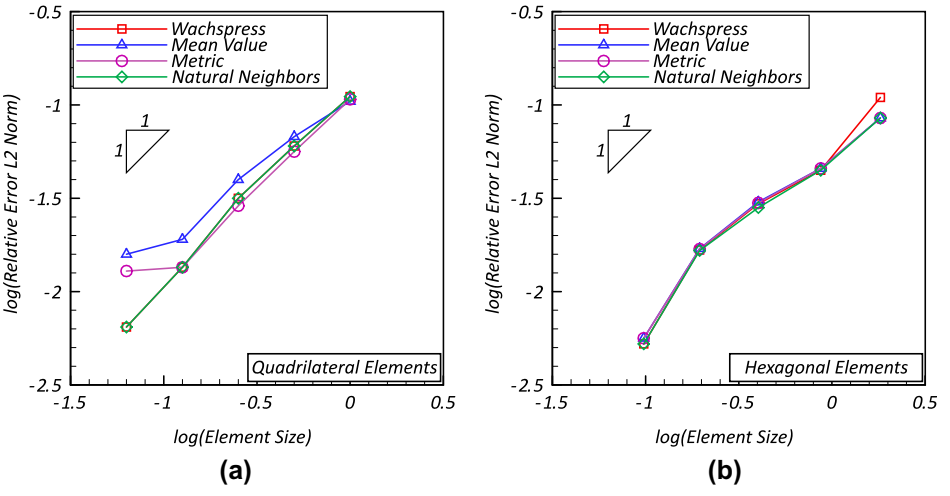

Figure 11. The variation of relative $L2$ error norm of displacement with element size for a rectangular plate with inclined interface using various polygonal interpolation functions: (a) quadrilateral elements and (b) hexagonal elements.

77, 281 and 1073 hexagonal elements are employed, as shown in Figure 10. Since the exact solution is not available for a comparison, a FE analysis with very fine mesh is carried out as a reference solution to illustrate the applicability of the proposed model in a problem with arbitrary material interface. In Figure 11, the variation of relative L2 error norm of displacement vs. the element size is plotted with respect to the reference solution on a log–log plot using various polygonal interpolation functions for both the quadrilateral and hexagonal elements. Obviously, the convergence rates of the Wachspress interpolation functions and natural neighbour-based functions are almost identical and more accurate than other two techniques. Clearly, it can be seen that the hexagonal elements result in a better convergence rate than the quadrilateral elements.

5.2. *Die-pressing with flexible central core*

The second example refers to die pressing of a rectangular plate with flexible central core, as shown in Figure 12. The component is restrained at the top edge, and a uniform deformation is imposed at the bottom up to 1.0 cm. The component is assumed to be elastic with the Young modulus of $2 \times 10^6\,\mathrm{kg/cm^2}$ and Poisson ratio of .35. The flexible central core has the elasto-plastic behaviour with the Young modulus of $2 \times 10^5\,\mathrm{kg/cm^2}$, Poisson ratio of .35, yield stress of $2400\,\mathrm{kg/cm^2}$ and the von-Mises plasticity with hardening parameter of $3 \times 10^5\,\mathrm{kg/cm^2}$. Two uniform non-conformal meshes of 1000 quadrilateral elements and 1086 hexagonal elements are employed for the polygonal–FEM analyses, as shown in Figure 13. In order to perform a real comparison, a fine conformal FEM mesh is applied as a reference solution with 1880 triangular elements for the FEM analysis. In the polygonal–FEM technique, those quadrilateral and hexagonal elements cut by the interface are decomposed into various polygonal sub-elements, and the polygonal-FEM analysis is carried out using the Wachspress method. The deformed configuration of the polygonal–FEM and standard–FEM solutions are presented in Figure 14 at the deformation of .7 cm. In Figure 15,

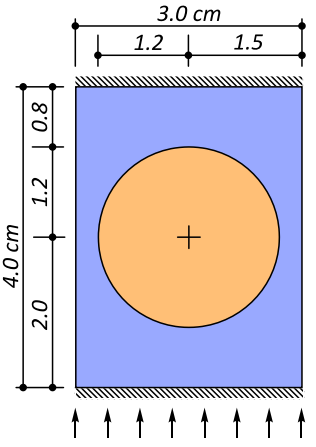

Figure 12. Die-pressing with a flexible central core; problem definition.

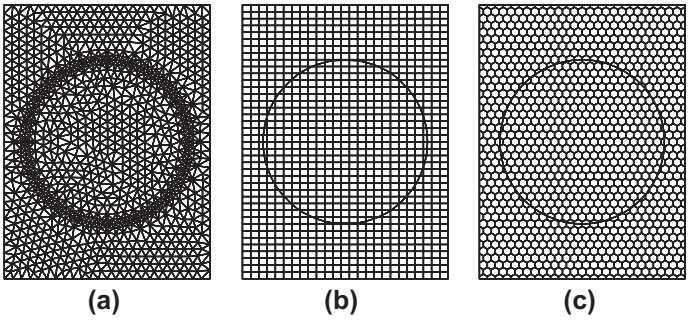

Figure 13. Die-pressing with a flexible central core: (a) FEM mesh of 1880 triangular elements, (b) polygonal–FEM mesh of 1000 quadrilateral elements and (c) polygonal–FEM mesh of 1086 hexagonal elements.

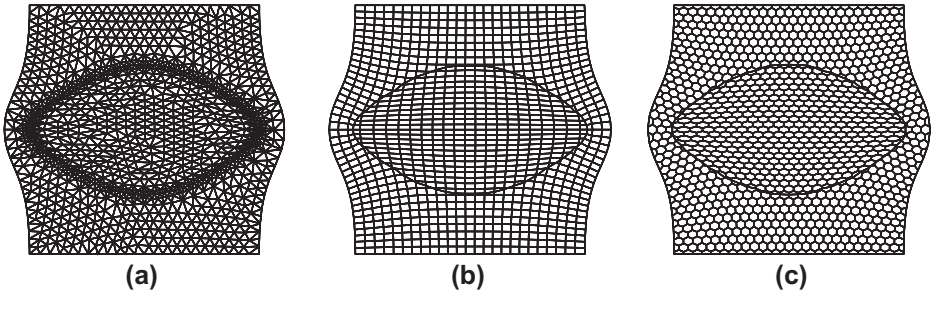

Figure 14. Deformed configurations at .7 cm: (a) FEM mesh of 1880 triangular elements, (b) polygonal–FEM mesh of 1000 quadrilateral elements and (c) polygonal–FEM mesh of 1086 hexagonal elements.

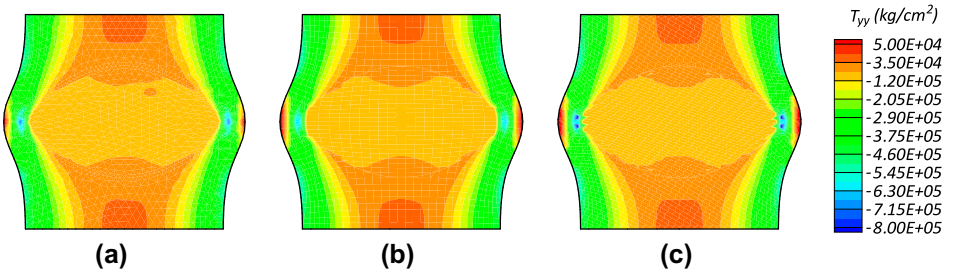

Figure 15. The distribution of normal stress contours at .7 cm: (a) FEM mesh of 1880 triangular elements, (b) polygonal–FEM mesh of 1000 quadrilateral elements and (c) polygonal–FEM mesh of 1086 hexagonal elements.

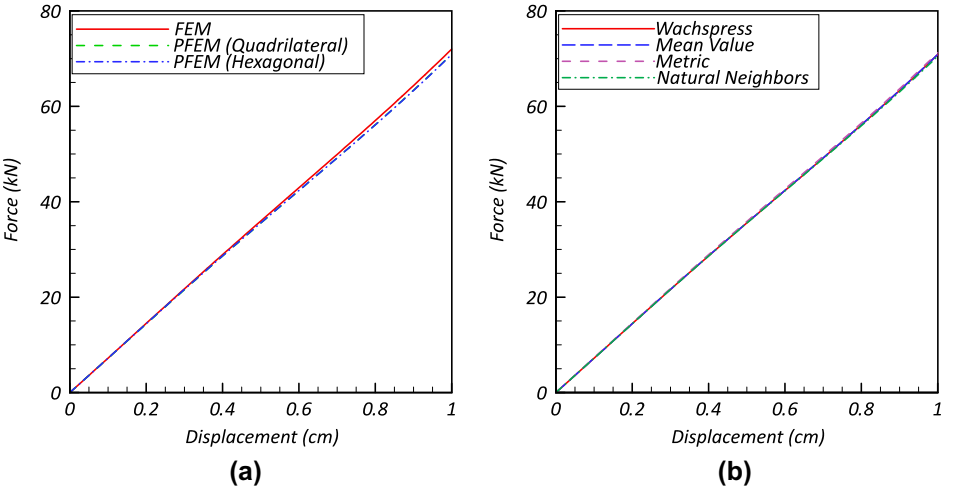

Figure 16. The variations of reaction force with vertical displacement: (a) a comparison between the FEM and polygonal–FEM techniques and (b) a comparison between the various polygonal shape functions.

the distribution of normal stress σ_y contours are presented for both polygonal–FEM and standard–FEM techniques at the final die-pressing. A comparison of the reaction force vs. vertical displacement is performed in Figure 16(a) between the polygonal–FEM method with quadrilateral mesh, the polygonal–FEM method with hexagonal mesh and the standard–FEM technique. Clearly, a good agreement can be seen between the polygonal–FEM and standard–FEM methods. Also plotted in Figure 16(b) is a comparison among various polygonal shape functions performed for the hexagonal mesh, i.e. the Wachspress interpolation functions, the metric coordinate shape functions, the natural neighbour-based functions and the mean value coordinate functions. It is noteworthy to highlight that although different approaches are used to construct the polygonal shape functions, all techniques result in a similar force–displacement curve, as shown in Figure 16(b). However, the convergence of non-linear polygonal–FEM solution in the metric coordinates method is more stable than other techniques.

5.3. *Pressing of rectangular plate with a central hole*

The next example refers to pressing of a rectangular plate with the circular hole, as shown in Figure 17. The plate is restrained at the top edge, and a uniform deformation is imposed at the bottom up to 1.0 cm. The plate is assumed to be elastic with the Young modulus of 2×10^6 kg/cm^2 and Poisson ratio of .35. Two uniform non-conformal meshes of 1000 quadrilateral elements and 1086 hexagonal elements are employed for the polygonal–FEM analyses, as shown in Figure 18. Moreover, a fine conformal FEM mesh is employed as a reference solution with 1802 triangular elements for the FEM analysis. In polygonal–FEM models, the uniform non-conformal meshes are decomposed into polygonal sub-elements that conform to the material interface, as shown in Figure 18(b–c). Obviously, the elements and sub-elements of circular hole that are not within the material zone are removed from polygonal–FEM meshes to perform the numerical analyses. The polygonal–FEM analyses are carried out using the Wachspress interpolation functions. The deformed configurations are presented in

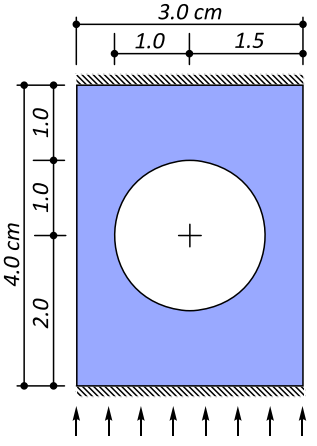

Figure 17. Pressing of rectangular plate with a circular hole; problem definition.

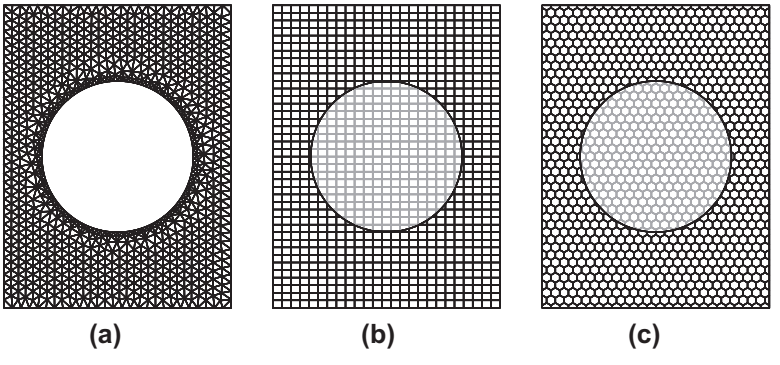

Figure 18. Pressing of rectangular plate with a circular hole: (a) FEM mesh of 1802 triangular elements, (b) polygonal–FEM mesh of 1000 quadrilateral elements and (c) polygonal–FEM mesh of 1086 hexagonal elements (number of elements in polygonal–FEM meshes are given before elimination of those elements that are not within the material zone).

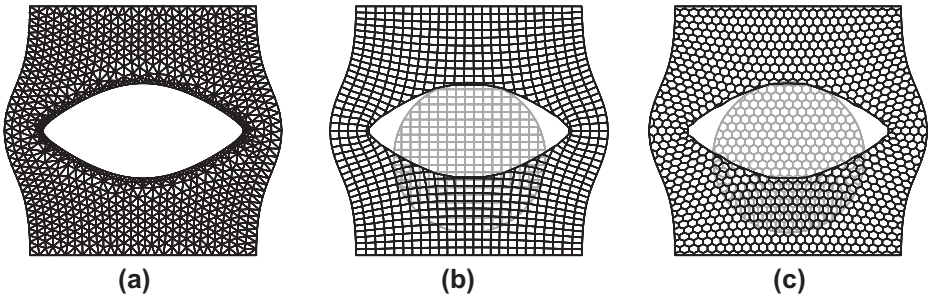

Figure 19. Deformed configurations at .7 cm: (a) FEM mesh of 1802 triangular elements, (b) polygonal–FEM mesh of 1000 quadrilateral elements and (c) polygonal–FEM mesh of 1086 hexagonal elements.

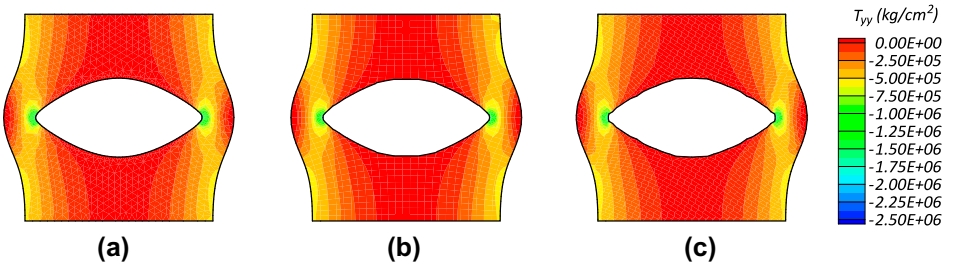

Figure 20. The distribution of normal stress contours at .7 cm: (a) FEM mesh of 1802 triangular elements, (b) polygonal–FEM mesh of 1000 quadrilateral elements and (c) polygonal–FEM mesh of 1086 hexagonal elements.

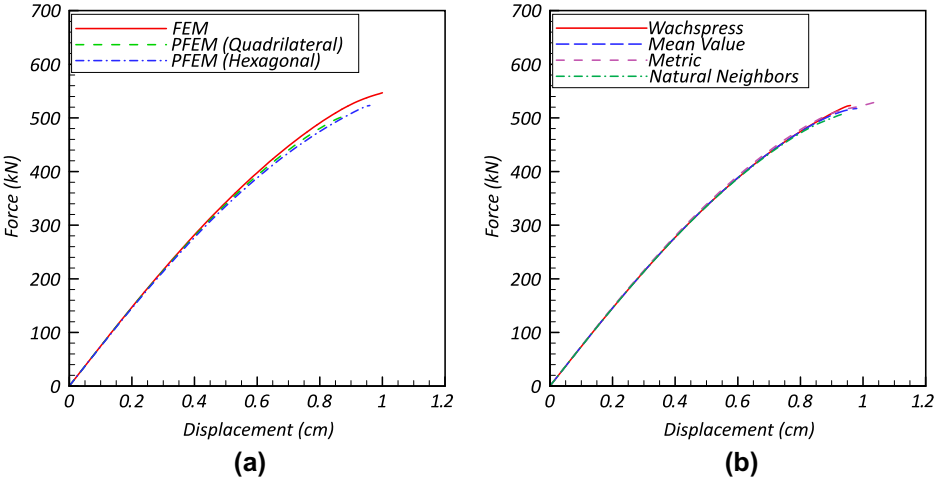

Figure 21. The variations of reaction force with vertical displacement: (a) a comparison between the FEM and polygonal–FEM techniques, and (b) a comparison between the various polygonal shape functions.

Figure 19 for the polygonal–FEM and standard–FEM techniques at the deformation of .7 cm. In Figure 20, the contours of normal stress σ_y are shown for both techniques at the final die-pressing. A comparison of the reaction force vs. vertical displacement is plotted in Figure 21(a) between the polygonal–FEM method with quadrilateral and hexagonal meshes, and the standard–FEM technique. Moreover, a comparison among various polygonal shape functions is performed in Figure 21(b) for the hexagonal mesh. Clearly, a good agreement can be seen between the standard–FEM method and the polygonal–FEM technique with different polygonal shape functions. This example adequately demonstrates the capability of proposed approach in modelling large plastic deformation with multiple material interfaces.

5.4. An elastic curved beam

The last example refers to the large deformation modelling of an elastic curved beam, as shown in Figure 22. The curved beam is fixed at the bottom, and a point load is applied at the free top end. The beam is assumed to be elastic with the Young modulus of $2 \times 10^6\,\mathrm{kg/cm^2}$ and Poisson ratio of .35. Two uniform non-conformal meshes of 1000 quadrilateral elements and 1086 hexagonal elements are used in the polygonal–FEM analyses, as shown in Figure 23. Moreover, a fine conformal FEM mesh of 302 triangular elements is employed as a reference solution in the FEM analysis. It must be noted that in polygonal–FEM models, the non-conformal quadrilateral and hexagonal grids are decomposed into sub-elements, in which the geometry of interface is used to produce various polygonal elements at the intersection of interface and the extra degrees-of-freedom are defined along the interface. Furthermore, the elements and sub-elements that are not within the material zone of the beam are removed, and the polygonal–FEM models are analysed under the prescribed point load. The polygonal–FEM analyses are carried out using the Wachspress interpolation functions. The deformed configurations of the polygonal–FEM method with quadrilateral and hexagonal meshes and the standard–FEM method are shown in Figure 24 at the vertical deformation of 3.5 cm. In Figure 25, the distribution of normal stress σ_y contours are presented for both techniques at the final stage of loading. A good agreement can be seen between two approaches. Finally, a comparison of the reaction force vs. vertical displacement is

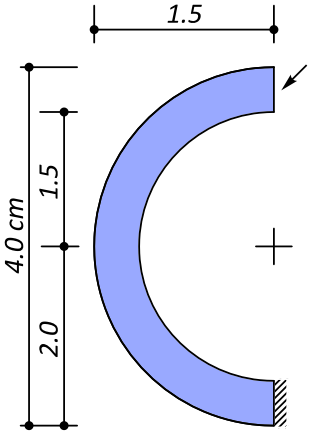

Figure 22. An elastic curved beam; problem definition.

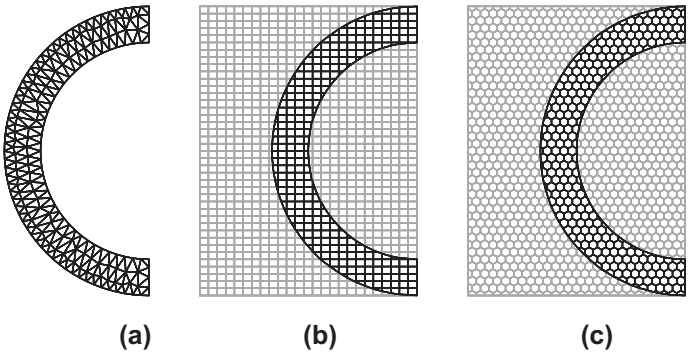

Figure 23. An elastic curved beam: (a) FEM mesh of 292 triangular elements, (b) polygonal–FEM mesh of 1000 quadrilateral elements and (c) polygonal–FEM mesh of 1086 hexagonal elements (number of elements in polygonal–FEM meshes are given before elimination of those elements that are not within the material zone).

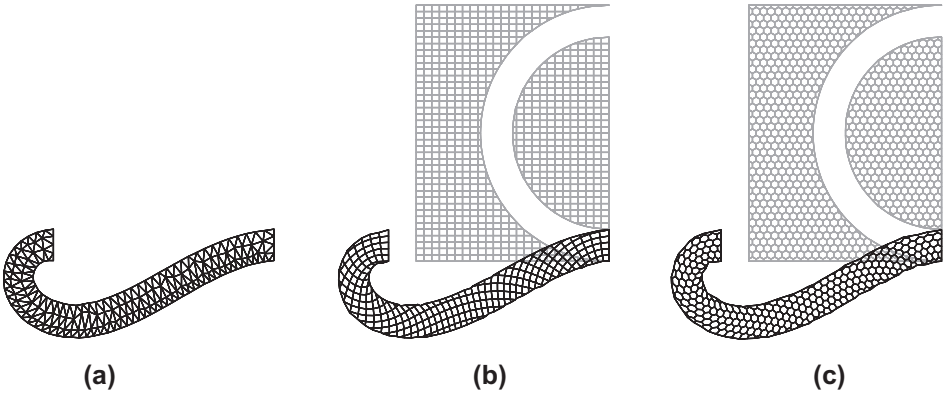

Figure 24. Deformed configurations at the vertical deformation of 3.5 cm: (a) FEM mesh of 292 triangular elements, (b) polygonal–FEM mesh of 1000 quadrilateral elements and (c) polygonal–FEM mesh of 1086 hexagonal elements.

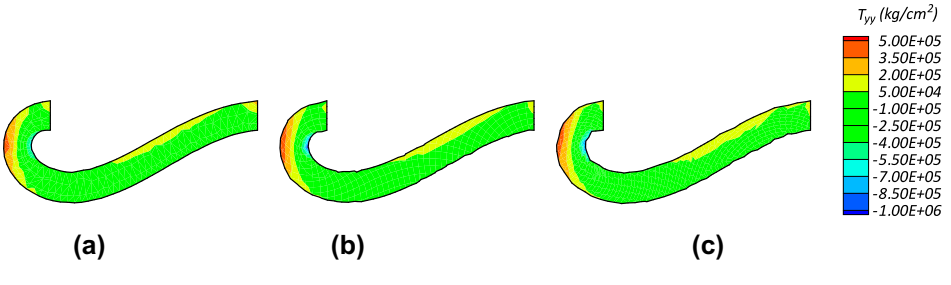

Figure 25. The distribution of normal stress contours at the vertical deformation of 3.5 cm: (a) FEM mesh of 292 triangular elements, (b) polygonal–FEM mesh of 1000 quadrilateral elements and (c) polygonal–FEM mesh of 1086 hexagonal elements.

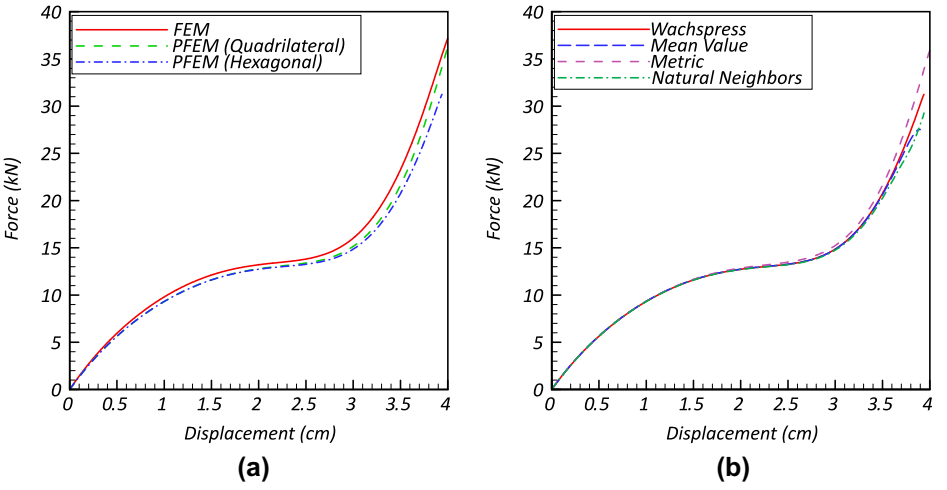

Figure 26. The variations of reaction force with horizontal displacement: (a) a comparison between the FEM and polygonal–FEM techniques, and (b) a comparison between the various polygonal shape functions.

performed in Figure 26(a) between the polygonal–FEM method with quadrilateral and hexagonal meshes, and the standard–FEM technique. Moreover, a comparison among various polygonal shape functions, i.e. the Wachspress, mean value, metric and natural neighbours shape functions, is performed in Figure 26(b) for the hexagonal mesh. It was observed from this example once again that the metric coordinates method exhibit a stable convergence of global error in the non-linear solution of large deformation polygonal–FEM analysis compared to other techniques.

6. Conclusion

In the present paper, the performance of polygonal–FEM method was investigated in modelling of large deformation problems based on various polygonal shape functions, including the Wachspress interpolation functions, the metric coordinate shape functions, the natural neighbour-based functions and the mean value coordinate functions. The polygonal–FEM method was employed on the basis of conformal decomposition on non-conformal meshes, in which the new conforming sub-elements were generated in the uniform structured mesh that conform to the internal interfaces. The geometry of interface was used to produce various polygonal elements at the intersection of interface with regular FE mesh, in which the extra degrees-of-freedom were defined along the interface. The level set method was employed to describe the material geometry on the background mesh by extruding arbitrary geometry from an initial background mesh. By defining the material interface in the non-conformal mesh and performing the conformal decomposition to generate various polygonal sub-elements, the standard elements and conformal sub-elements within the material zone were determined, and those elements or sub-elements which are not within the material zone were removed. Finally, the accuracy and versatility of various polygonal interpolation functions were investigated in the polygonal–FEM analysis of large deformation problems. Several numerical examples were solved using the polygonal–FEM method with quadrilateral and

hexagonal meshes and the results were compared with the standard–FEM method. The numerical convergence analysis was carried out for the polygonal–FEM method with quadrilateral and hexagonal meshes to study the approximation error and the convergence rate of various interpolation functions in polygonal elements. It was observed that the convergence rates of the Wachspress interpolation functions and natural neighbour-based functions are almost identical and more accurate than other two techniques. However, the metric coordinates method generally exhibits a stable convergence of global error in the non-linear solution of large deformation polygonal–FEM analysis compared to other techniques. The numerical results clearly demonstrate the capability of polygonal–FEM technique in modelling large plastic deformations with multiple material interfaces.

References

Anahid, M., & Khoei, A. R. (2008). New development in extended finite element modeling of large elasto-plastic deformations. *International Journal for Numerical Methods in Engineering, 75*, 1133–1171.

Belytschko, T., Krongauz, Y., Organ, D., Fleming, M., & Krysl, P. (1996). Meshless methods: An overview and recent developments. *Computer Methods in Applied Mechanics and Engineering, 139*, 3–47.

Belytschko, T., Moës, N., Usui, S., & Parimi, C. (2001). Arbitrary discontinuities in finite elements. *International Journal for Numerical Methods in Engineering, 50*, 993–1013.

Biabanaki, S. O. R., & Khoei, A. R. (2012). A polygonal finite element method for modeling arbitrary interfaces in large deformation problems. *Computational Mechanics, 50*, 19–33.

Coxeter, H. S. M. (1961). *Introduction to geometry*. New York, NY: Wiley.

Dahmen, W., Dikshit, H. P., & Ojha, A. (2000). On Wachspress quadrilateral patches. *Computer Aided Geometric Design, 17*, 879–890.

Dalton, G. R. (1985). Automatic indexed calculation of Wachspress' rational finite element functions. *Computers & Mathematics with Applications, 11*, 625–641.

Dasgupta, G. (2003a). Interpolants within convex polygons: Wachspress' shape functions. *Journal of Aerospace Engineering, 16*, 1–8.

Dasgupta, G. (2003b). Integration within polygonal finite elements. *Journal of Aerospace Engineering, 16*, 9–18.

Dasgupta, G., & Wachspress, E. L. (2008). Basis functions for concave polygons. *Computers & Mathematics with Applications, 56*, 459–468.

Floater, M. S. (2003). Mean value coordinates. *Computer Aided Geometric Design, 20*, 19–27.

Gout, J. L. (1985). Rational Wachspress-type finite elements on regular hexagons. *IMA Journal of Numerical Analysis, 5*, 59–77.

Khoei, A. R., Anahid, M., & Shahim, K. (2008). An extended arbitrary Lagrangian–Eulerian finite element method for large deformation of solid mechanics. *Finite Elements in Analysis and Design, 44*, 401–416.

Khoei, A. R., Biabanaki, S. O. R., & Anahid, M. (2008). Extended finite element method for three-dimensional large plasticity deformations on arbitrary interfaces. *Computer Methods in Applied Mechanics and Engineering, 197*, 1100–1114.

Li, Z., Lin, T., & Wu, X. (2003). New Cartesian grid methods for interface problems using the finite element formulation. *Numerische Mathematik, 96*, 61–98.

Malsch, E. A., & Dasgupta, G. (2004a). Shape functions for polygonal domains with interior nodes. *International Journal for Numerical Methods in Engineering, 61*, 1153–1172.

Malsch, E. A., & Dasgupta, G. (2004b). Interpolations for temperature distributions: A method for all non-concave polygons. *International Journal of Solids and Structures, 41*, 2165–2188.

Malsch, E. A., Lin, J. J., & Dasgupta, G. (2005). Smooth two-dimensional interpolations: A recipe for all polygons. *Journal of Graphics, GPU, and Game Tools, 10*, 27–39.

Meyer, M., Barr, A., Lee, H., & Desbrun, M. (2002). Generalized barycentric coordinates on irregular polygons. *Journal of Graphics Tools, 7*, 13–22.

Moës, N., Cloirec, M., Cartraud, P., & Remacle, J. F. (2003). A computational approach to handle complex microstructure geometries. *Computer Methods in Applied Mechanics and Engineering, 192*, 3163–3177.

Natarajan, S., Bordas, S., & Mahapatra, D. R. (2009). Numerical integration over arbitrary polygonal domains based on Schwarz–Christoffel conformal mapping. *International Journal for Numerical Methods in Engineering, 80*, 103–134.

Noble, D. R., Newren, E. P., & Lechman, J. B. (2010). A conformal decomposition finite element method for modeling stationary fluid interface problems. *International Journal for Numerical Methods in Fluids, 63*, 725–742.

Pinkall, U., & Polthier, K. (1993). Computing discrete minimal surfaces and their conjugates. *Experimental Mathematics, 2*, 15–36.

Strouboulis, T., Copps, K., & Babuška, I. (2001). The generalized finite element method. *Computer Methods in Applied Mechanics and Engineering, 190*, 4081–4193.

Sukumar, N. (2004). Construction of polygonal interpolants: A maximum entropy approach. *International Journal for Numerical Methods in Engineering, 61*, 2159–2181.

Sukumar, N., Chopp, D. L., Moës, N., & Belytschko, T. (2001). Modeling holes and inclusions by level sets in the extended finite-element method. *Computer Methods in Applied Mechanics and Engineering, 190*, 6183–6200.

Sukumar, N., & Malsch, E. A. (2006). Recent advances in the construction of polygonal finite element interpolants. *Archives of Computational Methods in Engineering, 13*, 129–163.

Sukumar, N., & Tabarraei, A. (2004). Conforming polygonal finite elements. *International Journal for Numerical Methods in Engineering, 61*, 2045–2066.

Wachspress, E. L. (1975). *A Rational Finite Element Basis*. New York, NY: Academic Press.

Wachspress, E. L. (2011). Barycentric coordinates for polytopes. *Computers & Mathematics with Applications, 61*, 3319–3321.

Warren, J. (1996). Barycentric coordinates for convex polytopes. *Advances in Computational Mathematics, 6*, 97–108.